

# Specific Heat Of Doped High- $T_C$ Cuprate Superconductors Within The Bose-Fermi-Hubbard Model

\* Michael Nakitare Waswa

Department of Physical Sciences, University of  
Kabianga  
Kericho, Kenya  
Michaelnakitare439@gmail.com

Yudah Kennedy Ayodo

Department of Physical Sciences, Kaimosi  
Friends University College  
Kaimosi-Vihiga, Kenya

Thomas Welikhe Sakwa

Department of Physics, Masinde Muliro University  
of Science and Technology  
Kakamega, Kenya

Bonface Ndinya

Department of Physics, Masinde Muliro University  
of Science and Technology  
Kakamega, Kenya

**Abstract**—Studies on superconductivity arising from doping a Mott insulator have become critical in the area of superconductivity. Within the framework of the Bose-Fermi-Hubbard model, we discuss the thermodynamic phase transition via specific heat in hole and electron doped high- $T_C$  cuprate superconductors. By considering the interplay between the electrons (fermions) and cooper pairs (bosons), the main features of the temperature dependence of the specific-heat, are well reproduced. It is shown that a hump-like feature in the specific-heat appears at the superconducting transition temperature  $T_C$ , and then the specific-heat varies exponentially as a function of temperature for the temperatures  $T < T_C$ . This is in consistency that at lower temperatures, a superconducting gap seems to open progressively. In particular, quantitatively, we report a specific heat value  $\sim 4.6661 \times 10^{-3}$  eV/K for  $\text{YBa}_2\text{Cu}_3\text{O}_6$  (YBCO),  $4.6419 \times 10^{-3}$  eV/K for  $\text{La}_{2-x}\text{Sr}_x\text{CuO}_4$  (LSCO),  $4.67 \times 10^{-3}$  eV/K for  $\text{Nd}_{2-x}\text{Ce}_x\text{CuO}_4$  (NCCO) and  $4.662 \times 10^{-3}$  eV/K for  $\text{Pr}_{2-x}\text{Ce}_x\text{CuO}_4$  (PCCO) at their respective  $T_C$  values which are in favorable agreement with other recent research findings.

**Keywords**— Specific Heat; Superconducting Transition; Mott Insulator

## I. INTRODUCTION

Great insights towards understanding HTS have been made over the years of intense experimental and theoretical research on cuprate superconductors [1]. However, no general consensus on a specific microscopic pairing mechanism, capable of consistently explaining the complex phenomenology of the superconducting and normal states, has emerged. Since the discovery of cuprate high-temperature superconductors [2], electronic properties of a two-dimensional (2D) system near the Mott transition have attracted considerable attention, because the high-temperature superconductors are obtained by doping layered-structure Mott insulators with holes or electrons [3]. The anomalously high superconducting transition temperature ( $T_C$ ) is considered to be related to the

anomalous features near the Mott transition in a 2D system [4]. Because both hole-doped and electron-doped systems exhibit superconductivity, it is natural to consider that the mechanism of high- $T_C$  superconductivity is included in both cases [5]. Thus, a comprehensive understanding of the thermodynamic properties of hole-doped and electron-doped systems is desired in order to elucidate the mechanism of high- $T_C$  superconductivity. Among the highly unconventional properties of the cuprate superconductors are the d-wave symmetry of the superconducting gap and the presence of a pseudogap also with d-wave symmetry. Theoretical insight is provided by study of the low-energy excitations around the node in the d-wave gap, where low-temperature experiments including specific heat, transport, and penetration depth, together with angle-resolved photoemission spectroscopy are explored [6].

The Mott transition is a pervasive and complex phenomenon, observed in many correlated oxide systems [7]. It comes in two varieties: the bandwidth-controlled transition at half-filling, tuned by the ratio of the on-site Coulomb repulsion  $U$  and band width  $W$ , and the filling-controlled transition, tuned by electron doping  $x$  away from half-filling. Theoretically, Mott insulators exist only at half-filling: With one electron per site, hoppings necessarily create empty and doubly occupied sites that are heavily penalized by  $U$ . Introducing a finite charge density allows carriers to move without incurring the on-site Coulomb cost, destroying the Mott insulator [8]. However, owing to the effect of strong on-site Coulomb repulsion between the electrons, superconductivity in these systems may be quite different. Whereas in a conventional BCS superconductor, screening and retardation effects serve to minimize the role of Coulomb interaction, the role of the latter becomes crucial in a doped Mott insulator where the charge degrees of freedom are partially frozen by the severity of the Coulomb interaction. Strong arguments have been presented in the literature that a high temperature superconductor evolves from a Mott insulator doped by holes, and consequently the ground state can be very different from a conventional BCS state [9]. Several theoretical models have been advanced to explain the various properties of high- $T_C$  including the electronic models i.e one-band and three band models, Hubbard

models and the t-j models. These models provide an integral tool for studying the properties of such materials. The two-dimensional t-j model has been studied for many years as a model for the copper oxide planes found in high temperature superconductors. Despite considerable effort the basic thermodynamic properties of this model are still not well understood [10] and that its basic feature is still controversial due to its non-perturbative feature [4] which hinders the further understanding of the unconventional superconductivity [11].

The Hubbard model is a prototypical example of a strongly correlated system characterized by the competition between the strong particle interaction (U) and the kinetic energy (t). It is exactly solvable in one dimension, where the ground state at half filling is a Mott insulator for any repulsive non-zero interaction [12]. Despite the simplicity of the model, the physics arising in dimensions higher than one remains poorly understood. Different many-body approximations have been applied along the years in different lattice geometries and coupling regimes (U/t). Among them, let us cite Quantum and Variational Monte Carlo calculations, Dynamical Mean-Field Theory, Density Matrix Renormalization Group and, more recently, Density Matrix Embedding Theory [13]. However, all these approaches have shown their limitations to describe the strongly correlated regime of the Hubbard model (U/t >> 1), in spite of the significant computational cost of most of them [12]. While the Bose-Hubbard model takes care of the repulsive on-site interaction energy, Fermi Hubbard model contains attractive interaction energy, U in addition to their respective hopping terms. Thus, neither the Bose Hubbard model nor the Fermi Hubbard model can singularly and conclusively describe interacting particles in a doped High- $T_C$  cuprate system (containing free electrons or fermions and cooper pairs or bosons) and hence in this research we propose a hybrid model christened Bose-Fermi-Hubbard model that can effectively describe the dynamics of a doped cuprate. Fundamentally, we report on the temperature dependence of specific heat within the Bose-Fermi-Hubbard model for hole and electron doped cuprates.

Specific Heat is the amount of heat required to raise the temperature of a unit mass of substance by unit degree. From first law of thermodynamics, we have;

$$Q = dU + dW = dU + PdV \quad (1)$$

The specific heat at constant pressure and constant volume are:

$$C_P = \left(\frac{\partial Q}{\partial T}\right)_P = \left(\frac{\partial U}{\partial T}\right)_P \quad (2a)$$

And

$$C_V = \left(\frac{\partial Q}{\partial T}\right)_V = \left(\frac{\partial U}{\partial T}\right)_V \quad (2b)$$

The small difference between  $C_V$  and  $C_P$  can be negligible for lower temperatures, but for higher temperatures, it is very important since the rate of thermal expansion is high at high temperatures. We have considered  $C_V$  and assumed that the inter-atomic distance does not change during the heating process. Specific heat theories are summarized below [14].

#### a) Dulong and Petit's Law

Dulong and Petit's law states that the specific heat per gram atom of a crystal is  $C_V=3R = 5.96$  cal/mol, where

R is the universal gas constant. It is valid at room temperature and above but invalid at lower temperatures. According to Nernst, the specific heat tends to zero as the temperature approaches zero.

#### b) Einstein's Theory

According to Einstein's quantum theory, the specific heat at constant volume is;

$$C_V = 3Nk_B(\theta_E) \left[ \frac{e^{\theta_E}}{(e^{\theta_E}-1)^2} \right] \quad (3)$$

where  $\theta_E = (hv/k_B T)$  is the Einstein's temperature.

Einstein's theory explained the decrease in specific heat with decreasing temperature. But this decrease was more rapid than the experimentally observed value.

#### c) Debye's Theory

The specific heat at constant volume due to Debye's theory is given by;

$$C_V = \frac{3Nk_B}{x_m^3} \left[ 12 \int_0^{x_m} \frac{x^3 dx}{e^x - 1} - \frac{3x_m^4}{e^{x_m} - 1} \right] \quad (4)$$

where  $x = (\xi/k_B T)$ ,  $x = (\theta_D/T)$  and  $\theta_D$  is the Debye's temperature. It holds good for all substances except for graphite, bismuth, selenium and tellurium etc., and is valid for both higher and lower temperatures.

The heat capacity measurement of the specific-heat can probe the bulk properties of a superconductor, which has been proven as a powerful tool to investigate the low-energy quasi-particle excitations, and therefore gives information about the charge-carrier pairing symmetry, specifically, the existence of gap nodes at the Fermi surface [24].

In this paper, we start from this theoretical framework, and then provide an explanation to the temperature dependence of the thermodynamic specific heat in cuprate superconductors. We evaluate explicitly the specific heat and qualitatively reproduce some main features of the heat capacity on cuprate superconductors. In particular, we show the temperature dependence of specific heat has a hump-like feature at the superconducting (SC) transition temperature.

## II. FORMALISM

### A. Bose-Fermi-Hubbard Model

The two-dimensional Hubbard model [15] and the t-j model [16] are believed to capture the essential physics of HTSC. These models incorporate, the strongly correlated nature of the 3d electrons due to copper spins in  $\text{CuO}_2$  planes, but fail to account for the interaction between the cooper pairs and free electrons introduced as a result of doping. Doping introduces free electrons at the Fermi level of the superconductor which also interact among themselves and so to the cooper pairs within the crystal. The free electrons (fermions) could well be described by Fermi-Hubbard model while the interacting cooper pairs (bosons) are described by the Bose-Hubbard model. Cooper pair is a boson-like particle, and these (ground state) pairs only form in the vicinity of Fermi energy ( $E_F$ ). But Cooper pairs are composed of electrons, and these pairs are not bosons in a

real physical sense due to Cooper-pair formation mechanism. This means that, a Cooper pair as an independent boson-like entity cannot obey Fermi-Dirac (FDS) or Bose-Einstein (BES) statistics. However, the electrons in Cooper pairs do obey FDS [16]. In order to include these aspects, a hybrid model (Bose-Fermi Hubbard model) was constructed.

The Bose-Hubbard model in momentum space thus reads;

$$H_{B-H} = -J \sum_{\langle k, \sigma \rangle} (b_k^\dagger b_k + b_{-k}^\dagger b_{-k}) - \mu \sum_k b_k^\dagger b_k + \frac{U}{2} \sum_k b_k^\dagger b_k (b_k^\dagger b_k - 1) \quad (5)$$

The first term represents the kinetic energy of the bosons (cooper pairs),  $J$  is the super-exchange energy.  $J \geq 0$  denotes the strength of the nearest neighbour hopping term. The second term in equation (5) accounts for the chemical potential  $\mu$ , which fixes the particle number in the grand canonical ensemble. The third term is the repulsive interaction among bosons on the same lattice point. ( $U > 0$ ) is the magnitude of the on-site repulsion between the bosons.

The corresponding Fermi-Hubbard Hamiltonian is;

$$H_{F-H} = -t \sum_{k, -k} c_k^\dagger c_k - U \sum_k c_{k\uparrow}^\dagger c_{-k\downarrow}^\dagger c_{k\uparrow} - \mu \sum_k c_k^\dagger c_k \quad (6)$$

Where  $t$  is the hopping parameter,  $\mu$  is the chemical potential that determines the occupation of the band. The  $c_k^\dagger (c_k)$  are the fermionic creation (annihilation) operators.

### B. Diagonalization of the Bose-Fermi-Hubbard Model

Equations (5) and (6) are combined to obtain the Hamiltonian for the hybrid Bose-Fermi-Hubbard model.

$$H_{B-F-H} = -J \sum_{\langle k, -k \rangle} (b_k^\dagger b_k + b_{-k}^\dagger b_{-k}) - \mu \sum_k b_k^\dagger b_k + \frac{U}{2} \sum_k b_k^\dagger b_k (b_k^\dagger b_k - 1) - t \sum_{k, -k} c_k^\dagger c_k - U \sum_k c_{k\uparrow}^\dagger c_{-k\downarrow}^\dagger c_{k\uparrow} - \mu \sum_k c_k^\dagger c_k \quad (7)$$

Equation (7) was written in the formalism of second quantization by using the creation and annihilation operators (bosonic and fermionic) having momentum,  $k$  and spin  $\sigma$  and then constructed in terms of new creation-destruction operators' i.e Bogoliubov operators.

For the electron operators, we define new operators  $\gamma_k$  in terms of old operators,  $c_k$ ;

$$\gamma_k = u_k c_k - v_k c_{-k}^\dagger \quad (8a)$$

$$\gamma_{-k} = u_k c_{-k} + v_k c_k^\dagger \quad (8b)$$

There corresponding complex conjugates are;

$$\gamma_k^\dagger = u_k c_k^\dagger - v_k c_{-k} \quad (8c)$$

$$\gamma_{-k}^\dagger = u_k c_{-k}^\dagger + v_k c_k \quad (8d)$$

The  $\gamma$ 's are called quasi-particle annihilation (creation) operators. They fulfill the same fermionic anticommutation relations like the original operators so that they produce a complete set of fermionic excitations in one-to-one correspondence with the excitations of a normal metal and thus they are well-defined fermionic quasi-particles.

For the boson operators, we define new operators  $\mathcal{b}_k$  terms of old operators,  $b_k$ ;

$$\mathcal{b}_k = u_k b_k - v_k b_{-k}^\dagger \quad (9a)$$

$$\mathcal{b}_{-k} = u_k b_{-k} + v_k b_k^\dagger \quad (9b)$$

The complex conjugates for the boson operators are;

$$\mathcal{b}_k^\dagger = u_k b_k^\dagger - v_k b_{-k} \quad (9c)$$

$$\mathcal{b}_{-k}^\dagger = u_k b_{-k}^\dagger + v_k b_k \quad (9d)$$

The corresponding electronic and bosonic inverse transformation of equations (8) and (9) respectively and their conjugates are considered;

$$c_k = u_k \gamma_k + v_k \gamma_{-k}^\dagger \quad (10a)$$

$$c_{-k} = u_k \gamma_{-k} - v_k \gamma_k^\dagger \quad (10b)$$

$$c_k^\dagger = u_k \gamma_k^\dagger + v_k \gamma_{-k} \quad (10c)$$

$$c_{-k}^\dagger = u_k \gamma_{-k}^\dagger - v_k \gamma_k \quad (10d)$$

$$b_k = \mathcal{U}_k \mathcal{b}_k + \mathcal{V}_k \mathcal{b}_{-k}^\dagger \quad (11a)$$

$$b_{-k} = \mathcal{U}_k \mathcal{b}_{-k} - \mathcal{V}_k \mathcal{b}_k^\dagger \quad (11b)$$

$$b_k^\dagger = \mathcal{U}_k \mathcal{b}_k^\dagger + \mathcal{V}_k \mathcal{b}_{-k} \quad (11c)$$

$$b_{-k}^\dagger = \mathcal{U}_k \mathcal{b}_{-k}^\dagger - \mathcal{V}_k \mathcal{b}_k \quad (11d)$$

Substituting equations (10) and (11) in (7), generates a transformed effective Hamiltonian for the Bose-Fermi-Hubbard model

$$H_{B-F-H} = -t \sum_k (u_k^2 m_k + v_k^2 - v_k^2 m_{-k} + u_k v_k (\gamma_k^\dagger \gamma_{-k}^\dagger + \gamma_{-k} \gamma_k)) - U \sum_{k, k'} \{u_k v_k u_{k'} v_{k'} [m_{k'} + m_{-k'} - 1] (m_k + m_{-k} - 1) + u_k v_{k'} (1 - m_{k'} - m_{k'}) (u_k^2 \gamma_k^\dagger \gamma_{-k}^\dagger + \gamma_{-k} \gamma_k) - \gamma_{-k} \gamma_{k'}\} + 40T - \mu \sum_k (u_k^2 m_k + v_k^2 - v_k^2 m_{-k} + u_k v_k (\gamma_k^\dagger \gamma_{-k}^\dagger + \gamma_{-k} \gamma_k) - J \sum_k [2\mathcal{V}_k^2 + 2(\mathcal{U}_k^2 - \mathcal{V}_k^2) (n_k + n_{-k}) + 2\mathcal{U}_k \mathcal{V}_k (\mathcal{b}_k^\dagger \mathcal{b}_{-k}^\dagger + \mathcal{b}_{-k} \mathcal{b}_k)] - \mu \sum_k [\mathcal{V}_k^2 + (\mathcal{U}_k^2 - \mathcal{V}_k^2) (n_k + n_{-k}) + \mathcal{U}_k \mathcal{V}_k (\mathcal{b}_k^\dagger \mathcal{b}_{-k}^\dagger + \mathcal{b}_{-k} \mathcal{b}_k)] + \frac{U}{2} \sum_k \{[\mathcal{V}_k^4 + \mathcal{V}_k^2 (\mathcal{U}_k^2 - \mathcal{V}_k^2) (n_k + n_{-k}) + \mathcal{V}_k^2 \mathcal{U}_k \mathcal{V}_k (\mathcal{b}_k^\dagger \mathcal{b}_{-k}^\dagger + \mathcal{b}_{-k} \mathcal{b}_k) - \mathcal{V}_k^2] \quad (12)$$

The system energy is then obtained by invoking the constraint that the off-diagonal components degenerate to zero and the contribution of the forth-order terms is insignificant. The diagonal terms correspond to equilibrium states of the system and hence they are considered. Thus the ground state energy becomes;

$$\begin{aligned}
E_0 = & -t \sum_k (u_k^2 - v_k^2)(m_k + m_{-k}) + v_k^2 \\
& - U \sum_{k,k'} \{u_k v_k u_{k'} v_{k'} [m_k(1 - m_{k'}) \\
& - m_{-k} m_{-k'}] - u_k v_k u_{k'} v_{k'} [(1 - m_{-k})(1 \\
& - m_{k'}) + (1 - m_{-k})m_{-k'}]\} \\
& - \mu \sum_k (u_k^2 - v_k^2)(m_k + m_{-k}) + v_k^2 \\
& - J \sum_k 2v_k^2 + 2(u_k^2 - v_k^2)(n_k + n_{-k}) \\
& - \mu \sum_k [v_k^2 + (u_k^2 - v_k^2)(n_k + n_{-k})] \\
& + \frac{U}{2} \sum_{kk'} \{v_k^4 + v_k^2(u_k^2 - v_k^2)(n_k + n_{-k}) \\
& - v_k^2 + [v_k^2(u_k^2 - v_k^2)(n_k + n_{-k}) \\
& + (u_k^2 - v_k^2)(u_k^2 - v_k^2)(n_k \\
& + n_{-k}) - (u_k^2 - v_k^2)(n_k + n_{-k})\} \quad (13)
\end{aligned}$$

In order to diagonalize the Hamiltonian in equation (12), we put the sum of the off-diagonal terms equal to zero. By equating the coefficients of the off diagonal terms to zero, we obtain  $u_k = \sqrt{5}$  and  $v_k = 2$  by invoking the constraint (14);

$$u_k^2 - v_k^2 = 1 \quad (14)$$

Further still, at the lowest energy of the system, all occupation numbers;  $m_k, m_{-k}, n_k$  and  $n_{-k}$  decomposes to zero.

$$m_k = m_{-k} = 0; n_k = n_{-k} = 0 \quad (15)$$

Substituting the values of  $u_k$  and  $v_k$  alongside equation (15) simplifies the Hamiltonian to;

$$E_0 = -4t - 2\sqrt{5} \Delta - 8\mu + 8J + 6U \quad (16)$$

In order to inculcate temperature dependence into the system energy, the total energy is multiplied by the thermal activation factor  $e^{-\frac{\Delta \epsilon}{kT}}$ , where  $k$  is Boltzmann's constant and  $\Delta \epsilon$  is the energy gap. The energy gap for superconductors is a very small quantity and it is generally 1% of the minimum energy of the system [16]. Hence,  $\Delta \epsilon = 0.01E_0$ . At any temperature  $T$ , the energy of the system is given as;

$$E_T = E_0 e^{-\frac{E_0}{100kT}} \quad (17)$$

The first derivative of the energy of the system with respect to the temperature gives the specific heat at constant volume  $C_v$ . Using equation (17), specific heat is calculated as follows;

$$\begin{aligned}
C_v = \frac{\partial E_T}{\partial T} = \frac{\partial}{\partial T} \left\{ (-4t - 2\sqrt{5}\Delta - 8\mu - 8J \right. \\
\left. + 3U) e^{-\frac{(-4t - 2\sqrt{5}\Delta - 8\mu - 8J + 3U)}{100kT}} \right\} \quad (18a)
\end{aligned}$$

which simplifies to specific heat equation as;

$$\begin{aligned}
C_v = \frac{(-4t - 2\sqrt{5}\Delta - 8\mu - 8J + 3U)^2}{100kT^2} \\
e^{-\frac{(-4t - 2\sqrt{5}\Delta - 8\mu - 8J + 3U)}{100kT}} \quad (18b)
\end{aligned}$$

Equation (18b) is the expression for determining the specific heat for the Bose-Fermi-Hubbard system.

### III. RESULTS AND DISCUSSION

The cuprate total specific heat at constant volume  $C_v$  is the specific heat of the gas of Cooper-pairs (bosons) plus the specific heat of the gas of electrons (fermions). One of the characteristics quantities in the thermodynamic properties of cuprates is the specific heat, which can be obtained by evaluating the temperature-derivative of the internal energy as in equation (18a). In Fig. 1, we plot the specific heat  $C_v$  as a function of temperature for hole doped cuprates (YBCO and LSCO). The parameters used are  $t=0.44$  eV,  $U=12t$ ,  $J = 0.4t$ ,  $\mu=U/2$  and  $\Delta=1.6$  eV for YBCO and  $t=0.42$  eV,  $U=12t$ ,  $J = 0.4t$ ,  $\mu=U/2$  and  $\Delta=1.8$  eV for LSCO. The curves obtained for the Bose- Fermi-Hubbard hybrid model assume Gaussian nature. Similar curves were obtained by [17]; [18]; [19]; [20] and [21] while investigating specific heat as a function of temperature for different superconductors under different conditions. Apparently, the main feature of the specific-heat observed experimentally on the cuprate superconductors is qualitatively reproduced.

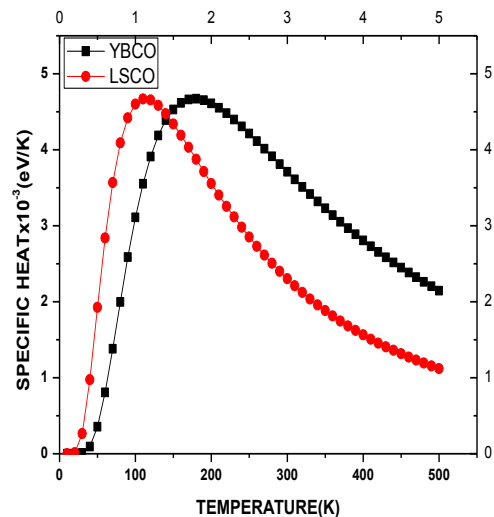


Figure 1: Variation of specific heat with temperature for YBCO and LSCO.

As can be seen from Fig. 1, the specific-heat anomaly (a jump) at  $T_c$  appears. At the peak ( $T=T_c$ ), the specific heat is  $4.6661 \times 10^{-3} \text{eV/K}$  ( $7.4658 \times 10^{-22} \text{JK}^{-1}$ ) and  $4.6419 \times 10^{-3} \text{eV/K}$  ( $7.4270 \times 10^{-22} \text{JK}^{-1}$ ) for YBCO and LSCO respectively. Hence our Bose-Fermi-Hubbard model gives an almost constant specific heat of  $7.0 \times 10^{-22} \text{JK}^{-1}$ . While studying the variation of specific heat with temperature for the t-J-d model [21] noted that the maximum heat capacity for YBCO and LSCO is  $4.7 \times 10^{-3} \text{eV/K}$  and hence the obtained values are in fine agreement. While investigating the interaction of Cooper pair and an electron for Y123 ( $T_c=93$  K), Bi2212 ( $T_c=95$  K), Hg1212 ( $T_c=128$  K) and Ti2212 ( $T_c=105$  K) [22] obtained a constant specific heat of  $4.5 \text{Jmol}^{-1} \text{K}^{-1}$  equivalent to  $7.472 \times 10^{-24} \text{JK}^{-1}$ . The SC transition is reflected by a peak in the specific-heat at  $T_c$ , however, the magnitude of the specific-heat decreases dramatically with decreasing temperatures for the

temperatures  $T < T_C$ . According to [22], the specific heat is fully determined by the low-lying excitation of super-fluid condensate. The low-lying condensate excitations are the quasi-particles. However, at low temperatures their contribution to the internal energy is exponentially suppressed. So that we are left with nodal quasi-electrons as the only relevant low-energy excitations in the superconductive phase at low enough temperatures. Customarily, the specific heat anomaly is characterized by  $\Delta C(T_C)$ , the difference of the specific heat between the peak value with respect to the background lattice specific heat. The essential physics of the hump-like anomaly of the specific-heat near  $T_C$  in cuprate superconductors in the low temperature regime can be attributed to the emergence of the normal-state pseudo-gap [22]. The steep reduction of  $C_V$  at  $T < T_C$  indicates that the energy gap grows rapidly below  $T_C$  and quasi-particle excitations are largely suppressed. These features suggest that the SC order parameter develops to a large extent at  $T > T_C$  but its phase fluctuates largely in the pseudo-gap regime. The peak value of the Gaussian curves represents the superconducting transition temperature of the hole-doped cuprates. At this point, a condensate is formed and  $C_V$  remains fairly constant. This depicts that the system is unstable at the peak and a second order phase transition (normal metal to superconducting state) occurs due absence of latent heat. It is vivid from the graphs that the  $T_C$  for YBCO is  $T_C \approx 171$  K which is higher than the experimental value of 92 K but close to the calculated value of 178 K. The graph for LSCO gives a  $T_C \approx 111$  K which is in fine agreement with the calculated value of 111 K. It is worth noting that the two values are in good agreement with the reported experimental value of 38 K.

Fig. 2 shows the graphs obtained using the Bose-Fermi-Hubbard model for NCCO and PCCO. The experimental values used are:  $t=0.42eV$ ,  $U=12t$ ,  $J = 0.4t$ ,  $\mu=U/2$  and  $\Delta=1.2eV$  for NCCO and  $t=0.38eV$ ,  $U=12t$ ,  $J = 0.4t$ ,  $\mu=U/2$  and  $\Delta=1.2eV$  for PCCO. The curves obtained are Gaussian mirroring those for YBCO and LSCO. We show that the specific-heat anomaly (a jump) appears at  $T_C$ , and then the specific heat varies exponentially as a function of temperature for the temperatures  $T < T_C$ . This is in consistency that at lower temperatures, a superconducting gap seems to open progressively. It is shown clearly that our present theoretical results capture all essential qualitative features of the doping dependence of the specific-heat observed experimentally on cuprate superconductors [23]. Like the hole doped cuprates, NCCO and PCCO equally have a hump-like turning point at  $T_C$ . According to [12], in the under-doped regime, the specific-heat jump near  $T_C$  is strongly suppressed, therefore there is no step-like specific-heat anomaly near  $T_C$ , instead, it shows a hump-like peak and remains as long tail. However, in the optimal doping, although the specific-heat anomaly is still not a sharp step-like, it shows a symmetric peak, and therefore there is a tendency towards to the step-like specific-heat anomaly with increasing doping. This tendency is particularly obvious in the over-doped regime, where the long tail appears in the under-doped regime becomes much shorter, and hence the specific-heat anomaly ends near  $T_C$  in the heavily over-doped regime, and a step-

like BCS transition with the absence of the long tail appears.

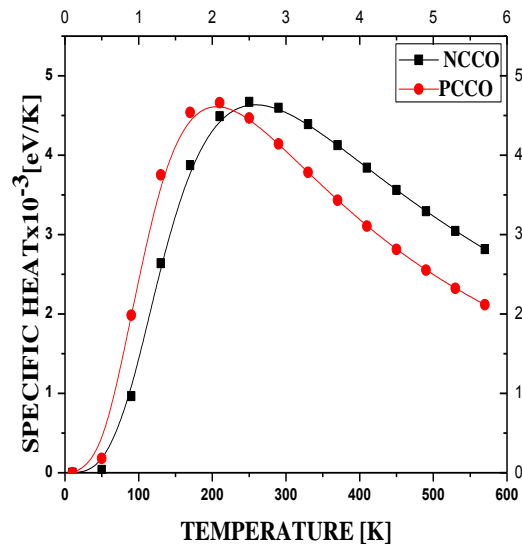


Figure 2: Variation of specific heat with temperature for NCCO and PCCO.

At the peaks, superconducting phase transition occurs and we can estimate  $T_C$  at this point. Peak specific heat occurs at critical temperature [24]. As expected the transition temperature corresponding to this phase transition is lower for PCCO compared to NCCO. The step-like transition occurs at  $T_C \approx 250$  K and  $T_C \approx 210$  K for NCCO and PCCO respectively. The values of specific heats corresponding to this jump are;  $C_V = 4.67 \times 10^{-3} eV/K$  ( $7.472 \times 10^{-22} JK^{-1}$ ) for NCCO and  $4.662 \times 10^{-3} eV/K$  ( $7.4592 \times 10^{-22} JK^{-1}$ ) for PCCO. Comparing with hole doped cuprates in this study, it worth to note that our model predicts comparable value of specific heat although at different transitional temperatures. However, both cuprates registered very high  $T_C$  values compared to their experimental values. The experimental value for NCCO is 24.5 K while that of PCCO is 19 K [25]. This result infers that a characteristic feature of the second order normal-superconductor phase transition is the jump in specific heat at  $T_C$  which is related to the release of entropy through the opening of the gap at the Fermi surface. At the peak ( $T=T_C$ ), the cuprates considered have an approximate  $C_V \sim 4.7 \times 10^{-3} eV/K$  which is in quantitative consonance with the findings of other authors. The specific heat discontinuity (jump) is proportional to the SC volume and its width mirrors the distribution of  $T_C$  within the whole volume. According to [26] the jump is experienced when specific heat is measured at a constant pressure and that lattice specific heat is considered not to change with the onset of superconductivity though it turns out to contribute more than 60%-70% [26] or more than 98% of total specific heat [27].

## CONCLUSIONS

The temperature dependence of specific heat at  $T < T_C$  is strongly reminiscent of that of a d-wave superconductor with line nodes in the gap and essentially different from that of an isotropic s-wave. We have explicitly demonstrated that superconductivity is a bulk phenomenon as exhibited by a hump-like feature on the specific heat

curve. The peak value of the Gaussian curves of specific heat represents the superconducting transition temperature of the cuprates. At this point, a condensate is formed and  $C_V$  remains fairly constant. This depicts that the system is unstable at the peak and a second order phase transition (normal metal to superconducting state) occurs due absence of latent heat. At their respective  $T_c$ 's the cuprates considered have an approximate  $C_V \sim 4.7 \times 10^{-3} \text{eV/K}$ . In general, the total specific heat of any system is the sum of several different excitations. Apart from fermionic specific heat driven by electrons, bosonic (driven by phonons and plasmons) specific heat need to be explored in order to unravel the magnitude of different contributions to the total specific heat. Investigating the contribution by phonons, for instance, could give information on the strength of electron-phonon coupling. The work on fermionic specific heat will be published later. The present formalism may be applied to other HTSC cuprates and to some iron-based superconductors, which will be considered in our future publication.

#### ACKNOWLEDGMENT

The authors would like to express their gratitude to Masinde Muliro University of Science and Technology for the opportunity and enabling environment to conduct this research.

#### REFERENCES

- [1] Leggett, A. J. What do we know about high  $T_c$ ? *Nature Phys.* 2, 134–136 (2006).
- [2] Bednorz, J. and Muller, K. . (1986). Possible High Temperature Superconductivity in the Ba-La-Cu-O System. *Nature Physics* . , 64 (2), 189-193.
- [3] Tokura, Y., Takagi, H., Uchida, S. (1989). A Superconducting Copper Oxide Compound with Electrons as the Charge Carriers. *Nature* . , 337, 345-347.
- [4] Lee, P. A., Nagaosa, N., and Wen, X.-G. (2006). Doping a Mott insulator: Physics of high-temperature superconductivity. *Rev. Mod. Phys* , 78, 7.
- [5] Kohno, M. (2014). Spectral properties near the Mott transition in the two-dimensional Hubbard model with next-nearest-neighbor hopping. *Physical Review B* , 90(3), 035111.
- [6] Newns, D. M., & Tsuei, C. C. (2007). Fluctuating Cu–O–Cu bond model of high-temperature superconductivity. *Nature Physics* , 3(3), 184-191.
- [7] Imada, M., Fujimori, A., and Tokura, Y. (1998). Metal-insulator transitions. *Rev. Mod. Phys* , 70, 1039.
- [8] Yee, C. H., & Balents, L. (2015). Phase separation in doped Mott insulators. *Physical Review X* , 5(2), 021007.
- [9] Weng, Z. Y., Zhou, Y., & Muthukumar, V. N. (2005). Bosonic resonating valence bond wave function for doped Mott insulators. *Physical Review B* , 72(1), 014503.
- [10] Putikka, W. O. (2015). Entropy and thermopower in the 2D t-J model. *Journal of Physics: Conference Series* , 640 (1), 012046.
- [11] Zhong, Y., Zhang, L., Lu, H. T., & Luo, H. G. (2015). Coexistence of antiferromagnetism and superconductivity of t't'-J model on honeycomb lattice. *Physica B: Condensed Matter* , 462, 1-7.
- [12] Zhao, J., Chatterjee, U., Ai, D., Hinks, D. G., Zheng, H., Gu, G. D., & Randeria, M. (2013). Universal features in the photoemission spectroscopy of high-temperature superconductors. *Proceedings of the National Academy of Sciences* , 110 (44), 17774-17777.
- [13] Knizia, G., and Chan, G. K. L. (2012). Density matrix embedding: A simple alternative to dynamical mean-field theory. *Phys. Rev. Lett* , 109, 186404.
- [14] Ramesh, N. A. (2016). Critical Studies on the Specific Heat of High Temperature Cuprate Oxide Superconductors. *International Journal of Advanced Research in Physical Science (IJARPS)* , 3 (4), 1-8.
- [15] Maier, T., White, J., Jarrell, M., Kent, P., Schulthess, T. (2005). New Insights into High Temperature Superconductivity from a Computational Solution of Two-Dimensional Hubbard Model. *Journal of Physics* , 16 (2005), 257-268.
- [16] Kaczmarczyk, J., Spalek, J., Schickling, T., and Bünemann, J. (2013). Superconductivity in the two-dimensional Hubbard model: Gutzwiller wave function solution. *Physical Review B* , 88 (11), 115127.
- [17] Khanna, K. (2008). Inaugural Lecture on Superconductivity. 7. Eldoret, Kenya: Moi University Press.
- [18] Yazici, D., Huang, K., White, B. D., Jeon, I., Burnett, V. W., Friedman, A. J and Maple, M. B . (2013). Superconductivity induced by electron doping in  $\text{La}_{1-x}\text{M}_x\text{OBiS}_2$  (M= Ti, Zr, Hf, Th) . *Physical Review B* , 87 (17), 174512.
- [19] Bhattacharyya, D. Adroja, N. Kase, A. Hillier, J. Akimitsu and A. Strydom. (2015). Unconventional Superconductivity in  $\text{Y}_5\text{Rh}_6\text{Sn}_{18}$  probed by Muon spin relaxation. *Scientific Reports* , 5, 1-8.
- [20] Abdel-Hafiez, M., Zhang, Y., He, Z., Zhao, J., Bergmann, C., Krellner, C., Duan, C., Lu, X., Luo, H., Dai, P., and Chen, X. (2015). Nodeless superconductivity in the present spin-density wave in pnictide superconductors: The case of  $\text{BaFe}_{2-x}\text{Ni}_x\text{As}_2$ . *Physical Review B* , 91, 1-10.
- [21] Rapando, B. W., Tonui J. K., Khanna K. M., and Mang'are, P. A. (2015). The diagonalized t-J Hamiltonian and the thermodynamic properties of High- $T_c$  superconductors. *American Research Journal of Physics (ARJP)* , 2016, 1-11
- [22] Odhiambo, J. (2016). Thermodynamic properties of high temperature superconductor cuprates due to interactions between cooper pairs and electrons. Doctorial Dissertation, Masinde Muliro University of Science and technology.
- [23] Paolo, C. (2016). The High Temperature Superconductivity in Cuprates: Physics of the Pseudogap Region. *European Physics Journa* , 1-55.
- [24] Ma, X., Qin, L., Zhao, H., Lan, Y., and Feng, S. (2016). Thermodynamic properties in triangular-lattice superconductors. *Journal of Low Temperature Physics* , 183 (5-6), 329-341.
- [25] Saxena K. A. (2010). *High Temperature Superconductors*. Berlin: Springer-Verlag.
- [26] Lin, J., and Millis, A. J . (2005). Theory of low-temperature Hall effect in electron-doped cuprates. *Physical Review B* , 72 (21), 214506.
- [27] Salas, P., Fortes, M., Solis, M. A., and Sevilla, F. J . (2016). Specific heat of Underdoped cuprate superconductors from a phenomenological layered Boson-Fermion model. *Physica C* , 524, 37-43.
- [28] Loram J. W., Mirza K. A., Cooper J. R., and Liang W. Y. (1993). Electronic specific heat of  $\text{Y123}$  from 1.8 to 300 K. *Physics Review Letters* , 71, 1740-1743.